RSC Advances

ROYAL SOCIETY OF CHEMISTRY

www.rsc.org/advances

Graphical abstract

Mechanical properties and structure of solvent processed novolac resin/layered silicate: development of interphase region

Parisa Jahanmard, Akbar Shojaei

Novolac/clay composites were prepared using solution mixing method. It was shown that the solution mixing method is able to disperse natural and organically modified clays in novolac resin efficiently. Development of strong interphase region around the silicated layers was explored. A micromechanical expression considering interphase region for intercalated morphology was proposed.

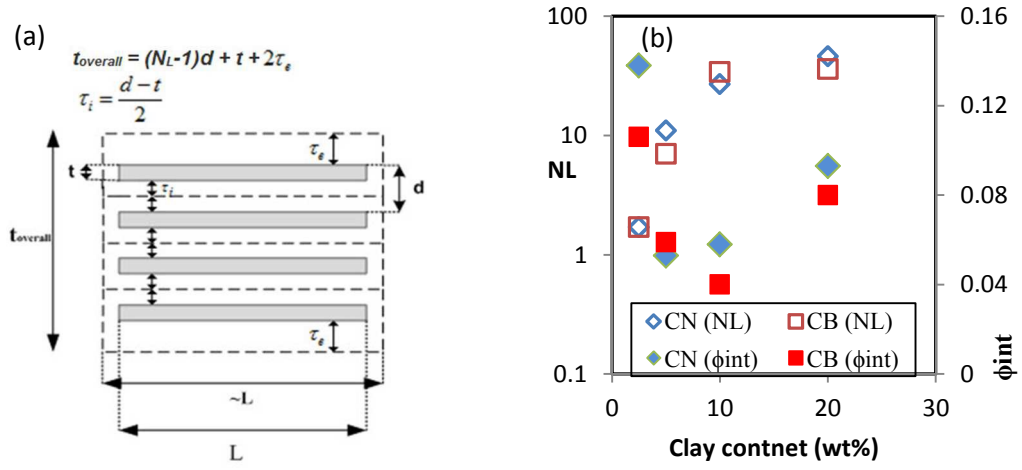

Mechanical properties and structure of solvent processed novolac resin/layered silicate: development of interphase region

Parisa Jahanmard, Akbar Shojaei*

Abstract

Composites of phenol-formaldehyde (PF) resin with Closite Na^+ and Closite 30B up to 20 wt% loadings were prepared by solution mixing. Tensile testing showed that both pristine and organically modified clays increased considerably the mechanical properties of PF resin at 2.5 wt% loading followed by marginal improvement or even sacrificed properties at high loadings. DMA and DSC analyses suggested development of highly crosslinked and well adhered interphase around silicate layers. A novel three-phase model considering the interphase region was proposed to predict composite modulus. The model was successfully employed to correlate morphological characteristics and mechanical properties of PF/clay composites.

Keywords: phenolic resin; clay; solution mixing; mechanical properties

Introduction

Phenol-formaldehyde (PF) resin is a kind of thermosetting polymer which has being used for a century. This polymer has found various applications in different areas such as molding compounds, laminates, composites, wood adhesive, foundry, coating, printed circuit boards, friction, abrasives, and insulation.[1,2] Such a wide range of applications for PF resin, so called phenolic resin, is originated from its good thermal stability, high ablative properties, good

Department of Chemical and Petroleum Engineering, Sharif University of Technology, P.O. Box 11155-9465, Tehran, Iran.

E-Mail address: akbar.shojaei@sharif.edu

solvent/chemical resistance, high electrical resistance, high char yield and good mechanical properties. Phenolic resin is commercially available in two different forms including resole and novolac whose synthesizing method differs in the phenol/formaldehyde ratio as well as polymerization reaction environments, i.e. acidic or basic conditions.[2]

Similar with many polymer nanocomposites, the incorporation of nanoparticles into the PF resin has also attracted the attention of researchers, targeting to obtain improved properties. Of various nanoparticles, nanoclay as the least expensive nanomaterials has been much considered in literature. Due to bulky, rigid and complex molecular structure of PF resin, the nanodispersion (intercalation/exfoliation) of clay in this matrix is not achieved easily. In order to improve the dispersibility of clay in the PF resin, many researchers have examined the role of mixing process, i.e. in situ polymerization, melt and solution, as well as the type of organic modifier of clay.[3-12] It is shown that the resole type phenolic resin which includes highly branched or three-dimensional molecular structure even at uncured state[7,9] is hardly suitable to intercalate into silicate gallery. Compared to resole, novolac resin is promising in obtaining much uniform nanodispersion of layered silicate because of the fact that this type may consist of linear molecular structure and its curing reaction is induced in presence of curing agent at elevated temperature, rather than the heat induced crosslinking reaction in the resole type.

Open literature indicates that research on the novolac resin/clay nanocompoistes is surprisingly sparse. The current works, dealing with this type of nanocomposite, have focused mostly on nanodispersion state and morphology, whereas the detailed mechanical properties analysis correlating with the microstructure of the nanocomposite has been seldom investigated. Literature shows that organically modified montmorillonite (MMT) can be dispersed uniformly and interact appropriately in novolac resin by melt mixing method [13,14] which often leads to

improved mechanical properties.[14] However, it was shown that this mixing process is not able to intercalate novolac resin into tactoids of pristine sodium MMT (Na^+MMT)[14] and only splitting of stacked silicate layers may be achieved in this case.[13] Therefore, melt processed novolac/Na^+MMT resulted in deterioration of mechanical properties of novolac resin.[14]

Recently, Zhang et al.[15] reported the morphological characteristics and thermal stability of low temperature curing novolac/clay nanocomposites with various organoclays and pristine clay prepared by solution high mixing process. Unlike to melt mixing process leading to poor dispersion of unmodified montmorillonite in novolac resin[8,14], they concluded that the biggest increment in d-spacing value is achieved in the case of unmodified clay (Na^+MMT) compared to other organocalys used in their study. This suggests that dispersion mechanism obtained by solution mixing method is possibly different from the melt mixing process. Unfortunately, Zhang et al.[15] did not report the mechanical properties of such solution processed clay filled nanocomposite, however, it appears that its mechanical properties may exhibit different characteristics with respect to melt processed samples.

Recently, we reported on the influence of clays on durability of PF/glass fiber composites.[16] The present research was focused on morphological characteristics and mechanical properties of novolac/clay composites to explore their structure-property relationship. A wide range of clay loadings up to 20 wt% was considered in this investigation to obtain deep insight into the role of state of dispersion of clays on the mechanical properties of PF/clay nanocomposites.

Experimental

Novolac phenolic resin (IP 502, hexamethylenetetramine, HMTA, of 8-10wt%, ρ=1.28 g/cm^3) produced by Resitan Co., Iran was employed. Closite®Na^+ abbreviated here by CN (natural

sodium pristine MMT with ρ =2.86 g/cm^3 and ignition loss 7 wt%) and Closite®30B abbreviated by CB (organically modified MMT with ρ=1.98 g/cm^3, modifier concentration 90 meq/100g and ignition loss 30 wt%) were supplied by Southern Clay Products, Inc.

Morphology of the nanocomposites and neat clays was examined by X-Ray diffraction (XRD) analysis using Philips diffractometer (40 kV, 30 mA, λ=17.9 nm, scanning rate of 0.02 °/s, Netherlands). The transmission electron microscopy (TEM) was carried out with a Philips CM-120 operating with an accelerating voltage of 120 kV on ultrathin sections prepared by diamond knife using OmU3 microtome (C. Reichert, Austria). The dynamic mechanical tests were performed using a Perkin–Elmer DMA 8000 analyzer on samples with dimensions 10×5×2 mm under bending mode at a fixed frequency of 1 Hz with temperature ramp of 5°C/min. Differential scanning calorimetric (DSC) analysis was performed on the uncured samples using TA-Instruments, DSC Q-100, USA, under nitrogen atmosphere at a heating rate of 10 °C/min. Mechanical properties were determined using a HIWA 2126 universal testing machine from HiwaEng, Co. Iran on rectangular specimens of 130×20×2 mm with a strain rate of 2 mm/min.

To prepare nanocomposites, novolac resin was first dissolved in methanol (99.8% purity, Merck) at ambient temperature using high speed mixer. Then the clays (both CN and CB) were added to this solution to obtain a concentration of 100 g (clay+resin)/200 cc solvent. The suspension is mixed for 10 min at 2000 rpm followed by sonication using Bandelin Sonorex (35 kHz) sonicator for 30 min at ambient temperature. Eventually, the compounds were dried at room temperature for 24 h followed by vacuum drying at 70° C for 2h to remove residual methanol and humidity. The loading of clays in the dried samples varied as 2.5, 5, 10 and 20 wt%. The dried samples were grounded in the form of fine powder to prepare the final test specimens using the compression molding.

All compounds were first pre-polymerized at 130°C for 6 min under vacuum to obtain B-staged samples. Then the B-staged samples were grounded as fine powder, poured into steel mold frame (200×130×2 mm) and hot pressed under 200 bars at 140°C for 8 min to fabricate PF/clay composites. Finally, to obtain fully postcured samples, the molded samples were postcured at a multistep heating program as: 150°C/6h (under vacuum)-160°C/2h-180°C/2h-200°C/2h. In order to examine the evolution of crosslinking appropriately, some typical samples were also partially postcured at a single heating step of 150°C/6h (under vacuum).

Results and discussion

Morphology

As shown in Fig. 1a, the d-spacing of neat CN increases from 1.19 nm to 1.49 nm at 2.5 wt% loading and then it is almost leveled off up to 10 wt% loading. However, at 20 wt% loading, a small decrease in d-spacing is observed, but its d-spacing value is still higher than that of neat CN. Such a trend in the d-spacing increment (Δd) with pristine sodium MMT (CN) loadings is completely consistent with solution processed novolac/CN mixture reported by Zhang et al.[15], showing the penetration of novolac molecules into the silicate gallery. The driving force for penetration of novolac molecules into the silicate gallery of unmodified CN is more likely the thermodynamic affinity between polymer-silicate layer originated from the hydroxyl groups of the novolac resin[2] and oxygen groups of natural silicate platelets.[17] However, such a thermodynamic affinity cannot solely be responsible for the intercalation of novolac resin as that was not observed in melt processing of novolac/CN.[14] The capability of solution process in intercalation of novolac resin even at high clay loading is supposed to be due to the initial increase of interlayer spacing of silicate gallery caused by the intercalation of methanol small

molecules. Additionally, the lower viscosity of novolac solution compared to the melt state can further facilitate the intercalation.

As shown in Fig. 1b, the d-spacing of neat CB powder is higher than that of CB dispersed in the PF matrix, while the peak intensity has reduced significantly. The reduction of peak intensity can be attributed to the conversion of some portion of clay gallery to single silicate layer (exfoliated morphology).[18] Furthermore, such a trend in shifting of XRD peaks is consistent with that of Zhang et al.[15] for CB loadings higher than 2.5 wt%. The decrease in d-spacing of gallery in polymer/organoclay systems has been reported previously for polymer nanocomposites which could be attributed to the exit of organic materials from the gallery caused by thermal degradation[19,20], compressive force exerted during processing[21] or extraction by solvent/polymer solution.[15] As the samples examined here were obtained by solution mixing process at low temperature, a possible reason for the decrease of d-spacing could be the extraction of organic materials by the solvent, i.e. the interaction of methanol with modifier and pulling it out. To examine such possibility, CB/methanol mixture (without the novolac resin) was prepared by the same mixing procedure as the novolac/CB/methanol mixture. Then the mixture was dried accordingly. The same experiment was also performed for CN as unmodified clay for the sake of comparison. These solvent processed clays were named as CN-SD and CB-SD for CN and CB, respectively.

As shown in Fig. 1, the peak position and the peak intensity of CN-SD and CB-SD do not change at all with respect to the corresponding original clays. This suggests that the methanol is unable to neither extracting the organic material of gallery nor breaking down of silicate stack (no change in the peak intensity) caused by the mechanical shearing. Therefore, a possible explanation of the d-spacing decrease for PF/CB could be the spatial rearrangement of organic

modifier within the silicate gallery, e.g. from paraffin-type arrangement to a lateral-type, upon entrance of novolac molecules after intercalation. Furthermore, the thermodynamic affinity between novolac resin and organic materials of CB could also lead to the partial extraction of organic modifier from the galley spacing which may be further reason for decrease of d-spacing.

Fig. 2 shows TEM micrographs of the fully post cured PF/clay composites at clay loading of 2.5wt%. Both exfoliated the intercalated morphologies are observed suggesting the formation nanocompoistes for both CN and CB filled PF.

Analysis of network structure using thermal transition characteristics

As shown in Figs. 3a,b, incorporation of the clays into novolac resin leads to a significant loss in tanδ peak value of novolac resin and an increment in its glass-transition temperature (T_g) associated with the tanδ peak position. These observations suggest that the segmental mobility of novolac resin has reduced significantly in presence of silicate layer[22-24] which is attributed to establishment of polymer-filler interaction at interface[24,25] leading often to development of a distinct interphase region with reduced macromolecular motion. However, for thermosetting polymers, like the novolac resin, the change in crosslinking density can also contribute to the segmental mobility of macromolecules reflecting in tanδ peak reduction and increment in T_g. As shown in Figs. 3c and d, above T_g where novolac resin is in rubbery state and its modulus is directly related to crosslinking density[26,27], effect of clay loading on the storage modulus was considerable and the role of each type of clay on this property was also distinguishable.

According to the theory of rubber elasticity, the elastic modulus of rubber materials is related directly to the crosslinking density as[27] $\upsilon_e = \frac{E_r}{3RT_r}$ where υ_e is the crosslinking density, E_r

the rubber modulus at the reference temperature T_r and R the universal gas constant. This model has been successfully employed to estimate the crosslink density of neat thermosetting resins[26] and thermosetting nanocomposite.[28] Table 1 represents the crosslinking density of novolac resin determined using rubber elasticity theory based on the procedure mentioned in literature.[26] It is revealed that the crosslink density of the novolac resin is enhanced greatly by incorporation of both types of clay.

Literature shows that unmodified clay (Na^+MMT) exhibited a positive influence on crosslinking density while organically modified clays did not act sensibly the same role on the crosslinking density of resole matrix. This behavior was attributed to the role of sodium cation (Na^+) in producing intermediate chelate promoting the addition of formaldehyde to phenol[12] or the role of pristine silicate in neutralizing partly the acid environment.[10] On the other hand, for the novolac resin/clay system prepared by melt mixing method where there was no HMTA inside the gallery, the DSC analysis has shown that clays did not affect the cure process.[8]

The significance of clay on the crosslinking density of novolac resin in our case could be explained by the conformational effect of novolac macromolecular chain on the curing process in presence of HMTA as described by Hirano and Yoshida.[2,29] According to them, reactive sites within the random coiled novolac molecules has less chance to take part in the curing reaction with respect to extended linear molecular structure leading to lower crosslinking density in random coiled state. In our case, it was postulated that novolac molecules within the silicate gallery got extended and become linear (at least in part) due to the spatial limitation in the gallery spacing, providing more crosslinks[2,29] whenever sufficient amount of HMTA is available in the gallery. As the novolac resin contained HMTA was used during the solution mixing, there was a chance to intercalate HMTA into the silicate gallery as well.

Additionally, novolac molecules are able to adhere (physically and/or chemically) to the surface of silicate layer due to the polarity of both novolac resin and the silicate layer surface, a fact that has already been addressed for the epoxy/layered silicate[30] and resol/layered silicate[10] systems. Such an interaction can also contribute to the extent of crosslinking density calculated by rubber elasticity theory. Consequently, difference in the crosslinking density of novolac resin in presence of unmodified and modified clays could possibly be associated to the difference in the degree of linearity of novolac resin within the silicate gallery and the amount of interaction between the silicate layer and novolac molecules. For the CB filled resin, it is thought that presence of organic modifier disturbs the linearity of molecules leading to lower crosslinking density. Moreover, the organic modifier provides higher free volume leading to less interaction between silicate layer and novolac molecules.

DMA curves of typical PF/clay composites which were partially postcured at 150°C/6h (under vacuum) were also determined to investigate further the network structure of novolac resin. As shown in Figs. 4a,b, tanδ curve of partially postcured samples is broad and in some cases it shows a shoulder. Meanwhile, tanδ peak height is greatly higher than that of the fully postcured samples shown in Fig. 3. As the postcuring process did not affect the dispersion state of clays, based on XRD data not shown here, the difference in the DMA results of fully and partially postcured samples could be attributed to the difference in the state of crosslinking in both cases. Figs. 4c,d show that storage modulus experiences a significant loss at T_g of novolac network followed by a rise at higher temperatures, i.e. above the regular T_g. The increment of storage modulus at higher temperatures could be attributed to the evolution of network structure and crosslinking density of partially postcured samples in the course of DMA experiment.[24, 31] Therefores, T_g value increases and it shifts to higher value leading to a broad tanδ-T curve.

It was tried to calculate the crosslinking density of partially postcured samples using rubber elasticity theory as it was performed for fully postcured samples. To do this, minimum storage modulus observed above T_g (corresponding to the first loss in storage modulus) was used to exclude the role of crosslink evolution at higher temperatures. As the extent of reduction of storage modulus in the first step loss of partially postcured sample is in the range of fully cured samples (compare Figs. 3c,d and 4c,d), it can be assumed that this minimum value for storage modulus is reasonably close to the rubbery state. Therefore, minimum storage modulus could be reasonable approximation for the storage modulus of rubbery state for partially postcured samples. This made possible the calculation of crosslinking density of as-partially postcured samples correctly. Furthermore, the T_g values of partially and fully postcured samples were extracted from the storage modulus versus temperature curves (the first loss in modulus curve) according to ASTM E 1640, since the tanδ curve showed broad peak for partially postcured samples making difficult extraction of the exact value of T_g from the tanδ peak position. Table 1compares the T_g value and crosslinking density of partially and fully postcured samples. As expected, the T_g and the crosslinking density increase substantially at fully postcured state. Moreover, it is found that the extent of increment in T_g, i.e. $\Delta T_g = T_g^F - T_g^P$, and υ_e, i.e. $\Delta \upsilon_e = \upsilon_e^F - \upsilon_e^P$, (where superscripts P and F stand for partially and fully postcured samples, respectively) of PF/clay samples upon completion of postcuring process are greater than those of neat novolac resin, i.e. greater than almost 10 ˚C for ΔT_g and 20000 mol/m^3 for $\Delta \upsilon_e$. This indicates the primary role of clays on the evolution of crosslink density and the interfacial interaction.

It is well established that the T_g of thermosetting polymer is linearly related to the crosslinking density as[26,27,32]

$$T_g = K\upsilon_e + T_{g_0} \quad (1)$$

where K is a constant and T_{g_0} is the glass transition temperature of the uncrosslinked resin. The constant K and T_{g_0} are determined from slope and intercept of T_g versus υ_e for each sample using the values obtained for partially and fully postcured samples. As given in Table 1, the slope K for the neat resin 0.0132 ºC.m^3/mol is of the range of values reported in literature[26,27,32], i.e. ~10^{-2}. Moreover, T_{g_0} of the neat uncrosslinked novolac resin obtained here (70.3 ºC) is consistent with that of novolac resin reported in literature.[8] Compared with the neat resin, the nanocomposites show significantly higher T_{g_0} while the slope K is lower, i.e. ~10^{-3}. To evaluate these results precisely, DSC thermograph of as-received novolac resin and uncured PF/clay nanocomposites were also determined. As shown in Fig. 5, narrow sharp endothermic peak appeared at 61.7 ºC is relevant to T_{g_0} of the neat novolac resin which is almost coincident with the value determined by Eq. (1). This supports the validity of Eq. (1) for the neat novolac resin. It is to be noted that the glass-transition behavior may be appeared as endothermic peak in DSC heat flow, rather than classical stepwise change. This behavior is basically observed only during the 1st heating run for amorphous polymers with T_g values above room temperature which are maintained for a long time in room temperature (aged in room temperature).

For PF/clay nanocomposites, two endothermic broad peaks are appeared in DSC thermographs. The first peak around 62 ºC is more likely relevant to the T_{g_0} of the novolac resin in the bulk. Even though the height of this peak has changed significantly but the peak position remains unchanged. The second endothermic broad peak, starting around 80 ºC, can possibly be attributed to the T_{g_0} of novolac resin molecules with restricted mobility which is more likely

adhered on the surface of the silicate layer, forming an interphase. The reduction of tanδ peak height of the pure novolac resin in presence of clays can be ascribed to the transfer of some portion of bulk resin to the regions of restricted mobility, i.e. interphase region, in the PF/clay composite. Such a dual T_g characteristic has been observed for other polymeric composites whenever a large interfacial area and good interfacial interaction are available.[33] Accordingly, it is revealed that the values of T_{g_0} for PF/clay composites obtained from the DSC are much lower than that of prediction by Eq. (1), see Table 1. This suggests that linear model is not valid for PF/clay composites and T_g varies nonlinearly with crosslinking density in this case possibly due to the fact that the composite includes a nonuniform network structure, i.e. bulk resin with normal crosslinking plus interphase region with highly crosslinked and severely adhered molecules to the silicate layers.

As shown in Fig. 5, incorporation of both clays shifts the cure temperature (exothermic peak around 130 °C) to lower values which could be ascribed to the catalytic role of silicate layer on the cure reaction of novolac resin. One possibility for this behavior may be the conformational change of novolac resin in the vicinity of silicate layer, as mentioned above according to DMA data, which increases the reaction site of novolac resin. The catalytic role of silicate layer on the cure process of thermosetting resin has been reported by others as well.[34]

Tensile properties

Fig. 6 exhibits mechanical properties of novolac resin filled with the clays. Tensile properties of PF/clay composite containing 2.5 wt% loadings of both clays are about 60% larger than those of pristine resin. Such a significant improvement could be attributed to the nanodispersion (intercalation/exfoliation) of clays within polymer matrix as well as the

formation of strong interphase between clays and resin.[6,14] A relative decrease in tensile properties over 2.5 wt% can be attributed to the suppression of nanodispersion state leading to promotion of agglomerates and stress concentration.[6] The slightly lower tensile properties of PF/CB composites compared with CN filled composites can be, at least in part, due to higher content of organic material in CB leading to a lower layered silicate content at the same weight percent of both clays. Furthermore, CN showed bigger effect on the promotion of crosslinking density as was discussed earlier which can aid to further improvement on mechanical properties.

It was attempted to compare experimental elastic modulus with the predictions obtained using two-phase micromechanical modeling based on Halpin-Tsai and Takayanagi models. For randomly oriented particulate reinforcements, Halpin-Tsai model is given as:[35-37]

$$\frac{E_c}{E_m} = \alpha \frac{1+\xi\eta_L\phi}{1-\eta_L\phi} + (1-\alpha)\frac{1+2\eta_T\phi}{1-\eta_T\phi} \qquad (2)$$

where $\eta_L = \frac{M-1}{M+\xi}$, $\eta_T = \frac{M-1}{M+2}$, E_c the elastic modulus of composite, ϕ the actual volume fraction of filler in the composite and ξ is a shape factor which is related to aspect ratio of the disk-like particles, i.e. ratio of length (l) to thickness (t), that is $\xi = 2(l/t)$. Here, M refers to the ratio of elastic modulus of reinforcing filler (E_f) to the matrix (E_m) and α is an orientation factor which takes the value of 0.49 for fully three-dimensional random orientation of disk-like reinforcements.[36] In addition, Takayanagi's model is expressed as follows:[38]

$$\frac{E_c}{E_m} = \left(1-\sqrt{\phi}+\frac{\sqrt{\phi}}{1-\sqrt{\phi}+\sqrt{\phi}\left(\frac{E_f}{E_m}\right)}\right)^{-1} \qquad (3)$$

In Eqs. (2) and (3), volume fraction of the clays was calculated based on the density of natural MMT. However, the volume fraction of CB was determined by excluding the organic content of the clay based on the ignition loss of CB reported by the manufacturer (see the experimental section) to obtain the volume fraction of neat silicate layer. This led to lower volume fraction of CB in the matrix compared to CN at similar weight percent.

In Halpin-Tsai model, the parameters E_f and ξ are often utilized as effective values depending on the intercalation/exfoliation state of clay in the matrix.[37] The elastic modulus and shape factor of a single silicate layer are 178 GPa and 200 (with length 100 nm and thickness 1 nm[35,37,39]), respectively, which can be used for fully exfoliated morphology. As a rough estimation, theoretical predictions for elastic modulus were performed by setting E_f and ξ in their maximum value as 178 GPa and 200, respectively. Even at this situation, theoretical predictions underestimate the experimental value at 2.5 wt% loadings (see Fig. 6). Such deviation can be attributed to the formation of considerable interphase region around the reinforcing particles as addressed by others for different polymer composites[40,41] as well. Furthermore, presence of interphase region was corroborated by DMA and DSC studies in previous section as well.

Ji's three-phase model considering the role of interphase region has been used frequently in literature[41,42], however, it appears to be useful for fully exfoliated system. In this study, a model is offered for the interphase region of a silicate layer in a stack, as shown schematically in Fig. 7a. According to this model, interphase region is divided into two parts including the internal interphase located between the gallery, and external interphase formed on the external surface of a stack. Due to the space limitation, the thickness of the internal interphase region (τ_i) is limited to the gap between two adjacent layers. The thickness of external interphase (τ_e) is

different than τ_i and depends on the radius of gyration of macromolecules which was considered to be 10 nm in this study.[41] Therefore, the total volume fraction of interphase region in the composite (ϕ_{int}) is the sum up the internal ($\phi_{int,i}$) and external ($\phi_{int,e}$) volume fractions. According to Fig. 7a, ϕ_{int} is directly related to the actual volume fraction of clay as $\phi_{int} = \frac{1}{N_L}[(\frac{d}{t}-1)(N_L-1)+2\frac{\tau_e}{t}]\phi$ where d is the d-spacing obtained by XRD for intercalated state, t the thickness of single silicate layer which is ~1 nm and N_L is the average number of silicate layer in a stack. Therefore, effective reinforcing particle (ERP) with uniform properties consisting of silicate layer and interphase regions is proposed to be used in the Halpin-Tsai model, as was performed in our previous work.[43] The effective modulus (E_{eff}) of ERP which may be obtained by the rule of mixtures is expressed as:

$$E_{eff} = [\frac{N_L t}{(N_L-1)d+t+2\tau_e}]E_s + [\frac{(d-t)(N_L-1)+2\tau_e}{(N_L-1)d+t+2\tau_e}]E_{int} \quad (4)$$

where E_s and E_{int} are the elastic modulus of the silicate layer and interphase region, respectively. In this study the mechanical properties of internal and external interphases were considered to be the same. Furthermore, volume fraction of the ERP is simply obtained by $\phi_{ERP} = \phi + \phi_{int} = \left[(1-\frac{1}{N_L})\frac{d}{t} + (1+\frac{2\tau_e}{t})\frac{1}{N_L}\right]\phi$. The equivalent shape factor for the ERP can also be expressed as $\xi = \frac{2l}{(N_L-1)d+t+2\tau_e}$.

In order to employ the concept of ERP in Halpin-Tsai equation, the E_{int} and the average number of silicate layer (N_L) must be known. The value of E_{int} was set to be 20 GPa which is consistent with literature.[41] Fig. 7b exhibits the variation of N_L and interphase volume fraction

(ϕ_{int}) versus the clay loadings. At 2.5 wt% loading, N_L is almost 2 for both CN and CB, indicating the nanodispersion of clays which is mainly the intercalated state, as shown in Fig. 2. Furthermore, the ϕ_{int} is considerably high at this clay content showing development of considerable interphase region. The thickness of gallery stack with two silicate layers is lower than gallery thickness observed by TEM (see Fig. 2), whereas overall thickness consisting of external interphase is calculated to be 22 nm which is almost consistent with microscopic observation. Moreover, it is observed that N_L increases dramatically and ϕ_{int} decreases considerably by increasing the clay loading which could be a consequence of the limited dispersion state of clays.

Conclusions

This study aimed at understanding correlation between the morphology and network structure with the mechanical properties of novolac resin/MMT composites prepared by solution mixing method. XRD and TEM analyses suggested the formation of intercalated morphology. It was shown that incorporation of both unmodified and organically modified clays led to dramatic reduction in tanδ peak height and increment of T_g of the resin. DMA observations and DSC analyses suggested that the incorporation of clays into novolac resin resulted in a nonuniform network structure including a bulk resin with normal crosslinking and interphase region surrounding a single platelet (silicate layer) with highly crosslinked structure. It was also postulated that novolac resin was able to interact with both natural and organically modified clays efficiently. Tensile testing showed that the clays loading increased the tensile strength and modulus of novolac resin considerably at 2.5 wt% loading (~60% increment) due to the nanodispersion of clays and good interfacial interaction and establishment of interphase region. A novel three-phase theoretical model based on the Halpin-Tsai equation considering interphase

in an intercalated stack was proposed. A good correlation was found between the modeling prediction and the morphological characteristics investigated by experimental techniques.

Acknowledgement

The financial support received from Iran National Science Foundation (INSF) for this research is gratefully acknowledged.

References

1 A. Knop and W. Scheib, *Chemistry and application of phenolic resins*, Springer-Verlag, Berlin, 1979.

2 Pillato L*, Phenolic resins: a century of progress*, Springer-Verlag, Berlin, 2010.

3 US Patent 4889885, 1989.

4 H. Wang, T. Zhao, L. Zhi, Y. Yan and Y. Yu, *Macromol. Rapid. Commun.,*2002, **23**:44-8.

5 H. Wang, T. Zhao, Y. Yan and Y. Yu*, J. Appl. Polym. Sci.,* 2004, **92,** 791-7.

6 J. Peppas, K. Patel and E. B. Nuaman, *J. Appl. Polym. Sci.,* 2005, **95**, 1169-74.

7 Z. Wu, C. Zhou and R. Qi, *Polym. Compos.,* 2002, **23**, 634-46.

8 M. H. Choi, I. J. Chung and J. D. Lee, *Chem. Matter.,* 2000, **12**, 2977-83.

9 H. Y. Byun, M. H. Choi and I. J. Chung*, Chem. Matter.,* 2001, **13**, 4221-26.

10 L. B. Manfredi, D. Puglia, JM. Kenny and A. Vazquez, *J. Appl. Polym. Sci.,* 2007, **104**, 3082-9.

11 C. C. Tasan and C. Kaynak, *Polym. Compos.,* 2009, **30**, 343-50.

12 L. B. Manfredi, D. Puglia, A. Tomasucci, J. M. Kenny and A. Vazquez, *Macromol. Mater. Eng.,* 2008, **293**:878-86.

13 M. H. Choi and I. J. Chung, *J. Appl. Polym. Sci.,* 2003, **90**, 2316-21.

14 S. G. Kang, J. H. Hong and C. K. Kim, *Ind. Eng. Chem. Res.,* 2010, **49**, 11954-60.

15 Z. Zhang, G. Ye, H. Toghiani and C. U. Pittman, *Macromol. Mater. Eng.,* 2010, **295**, 923-33.

16 M. Eesaee, and A. Shojaei, *Composites. Part A.,* 2014, **63**, 149-158.

17 S. Ravlidou and C. D. Papaspyrides, *Prog. Polym. Sci.,* 2008, **33**, 1119-98.

18 Kh. Khederlou, R. Bagheri and A. Shojaei, *Appl. Surf. Sci.,* 2014, **318**, 90-94.

19 T. Lan, P. D. Kaviratna and T. J. Pinnavaia TJ, *Chem. Mater.,* 1994, **6**, 573-5.

20 C. G. Martins, N. M. Larocca, D.R. Paul and L.A. pessan, *Polymer.,* 2009, **50**, 1743-54.

21 A. Behradfar, A. Shojaei and N. Sheikh, *Polymer Engineering & Science.,* 2010, **50**, 1315-25.

22 A. E. Gerbase, C. L. Petzhold and A. P. O. Costa, *Journal of the American Oil Chemists' Society (JAOCS).,* 2002, **79**, 797-802.

23 A. Shabeer, A. Garg, S. Sundararaman, K. Chandrashekhara, V. Flanigan and S. Kapila, *J. Appl. Polym. Sci.,* 2005, **98**, 1772-80.

24 S. G. Kuzak and A. Shanmugam, *J. Appl. Polym. Sci.,* 1999, **73**, 649-58.

25 V. M. Litvinov and P. A. M. Steeman, *Macromolecules.,* 1999, **32**, 8476-90.

26 J.S. Nakka, K. M. B. Jansen, L. J. Ernst and W. F. Jager, *J. Appl. Polym. Sci.,* 2008, **108**, 1414-20.

27 J. A. Schreoder, P. A. Madesen and R. T. Foister, *Polymer.,* 1987, **28**, 929-40.

28 O. Zabihi, A. Khodabandeh and S. M. Mostafavi, *Polym. Degrad. Stab.,* 2012, **97**, 3-13.

29 K. Hirano and T. Yoshida, Baekeland 2007 Centennial Symposium Ghent, September 23-6, 2007.

30 D. Wu, C. Zhou, X. Fan, D. Mao and Z. Bian, *Polym. Degrad. Stab.,* 2005, **87**, 511-19.

31 W. Stark, H. Goering, U. Michel and H. Bayerl, *Polymer Testing.,* 2009, **28**, 561-566.

32 L. E. Nielsen, *J MacromolSci Rev Macromol. Chem.,* 1969, **C3**, 69-103.

33 G. Tsagaropoulos and A. Eisenberg, *Macromolecules.,* 1995, **28**, 6067-77.

34 P. B. Messesmith and E. P. Giannelis, *Chem. Mater.,* 1994, **6**, 1719-25.

35 Y. Dong, D. Bhattacharyya and P.J. Hunter, *Compos. Sci. Technol.,* 2008, **68**, 2864-75.

36 M. A. Rafiee, J. Rafiee, Z. Wang, H. Song, Z. Yu and N. Koratkar, *ACS Nano.,* 2009, **3**, 3884-90.

37 T. D. Fornes and D. T. Pual, *Polymer.,* 2003, **44**, 4993-5013.

38 M. Takayanagi, S. Uemura and S. Minami, *J. Polym. Sci. Part C.,* 1964, **5**, 113-122.

39 H. Dalir, R. D. Farahani, V. Nhim and B. Samson, M. Levensque and D. Therriault, *Lamgmuir,* 2012, **28**, 791-803.

40 V. Cannillo, F. Bondioli, L. Lusvarghi, M. Montorsi, Avella M, M. E. Errico and M. Malinoconico, *Compos. Sci. Technol.,* 2006, **66**, 1030-7.

41 X. L. Ji, J. K. Jing, K. Jiang and B. Z. Jiang, *Polym. Eng. Sci.,* 2003, **42**, 983-93.

42 N. AitHocine, P. Mederic, and T. Aubry, *Polym. Test.,* 2008, **27**, 330-39.

43 M. M. Saatchi and A. Shojaei, *Mater. Sci. Eng A-Struct.,* 2011, **528**, 7161-72.

Table 1. DMA parameters and crosslinking density of partially and fully postcured samples.

Compound	υ_e^P (mol/m^3)	υ_e^F (mol/m^3)	T_g^P (˚C)	T_g^F (˚C)	T_{g0} (˚C)	K (m^3.˚C/mol)
PF	7028	10534	162.8	209	70.3	0.0132
PF/CN-2.5	5926	43869	169	224	160.4	0.0014
PF/CN-5	-	41940	-	231	-	-
PF/CN-10	13045	52467	167	228	146.1	0.0015
PF/CN-20	15834	78727	162.8	229	146.8	0.0011
PF/CB-2.5	5908	35708	168.4	223	157.5	0.0018
PF/CB-5	-	39298	-	228	-	-
PF/CB-10	10068	42764	179.2	239	160.8	0.0018
PF/CB-20	8592	25174	163.7	223	133	0.0036

T_{g0} is glass-transition temperature of uncured resin calculated using Eq. (1).

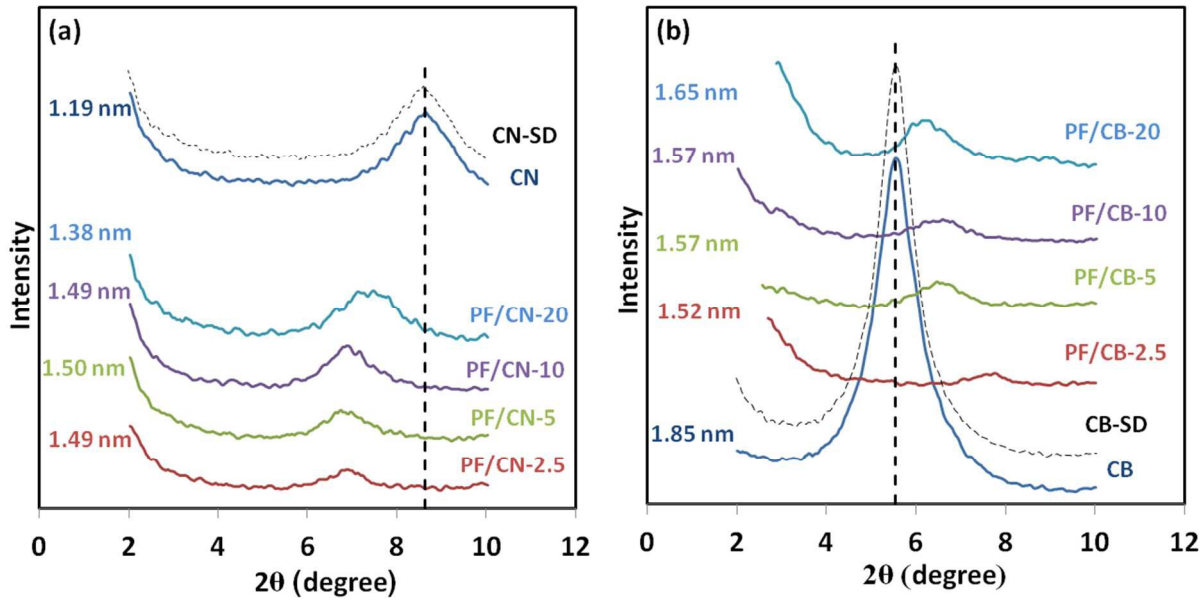

Fig. 1.Comparison of XRD pattern of uncured PF/clay composites with the corresponding neat clay; (a) PF/CN and (b) PF/CB.

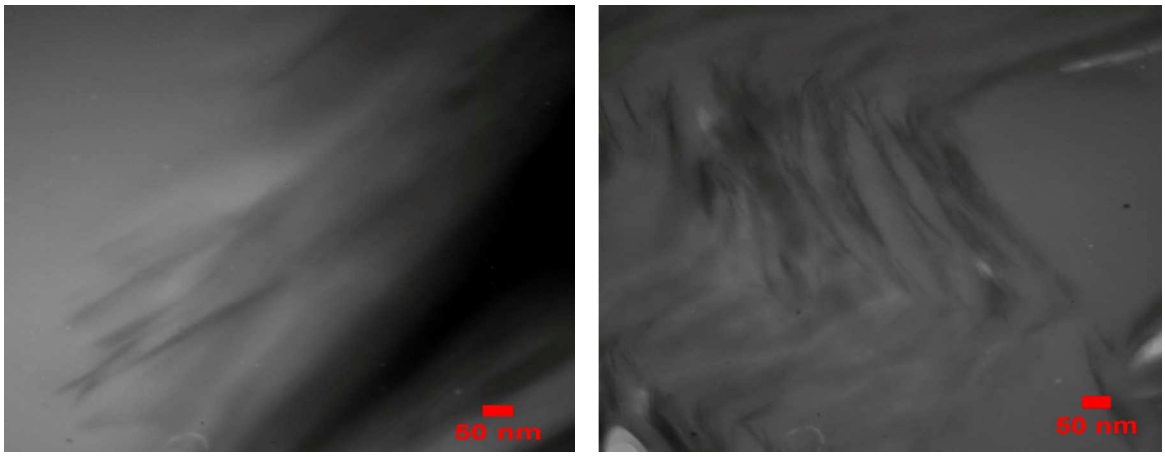

Fig. 2.TEM micrographs for (a) PF/CN and (b) PF/CB composites at 2.5 wt% loadings.

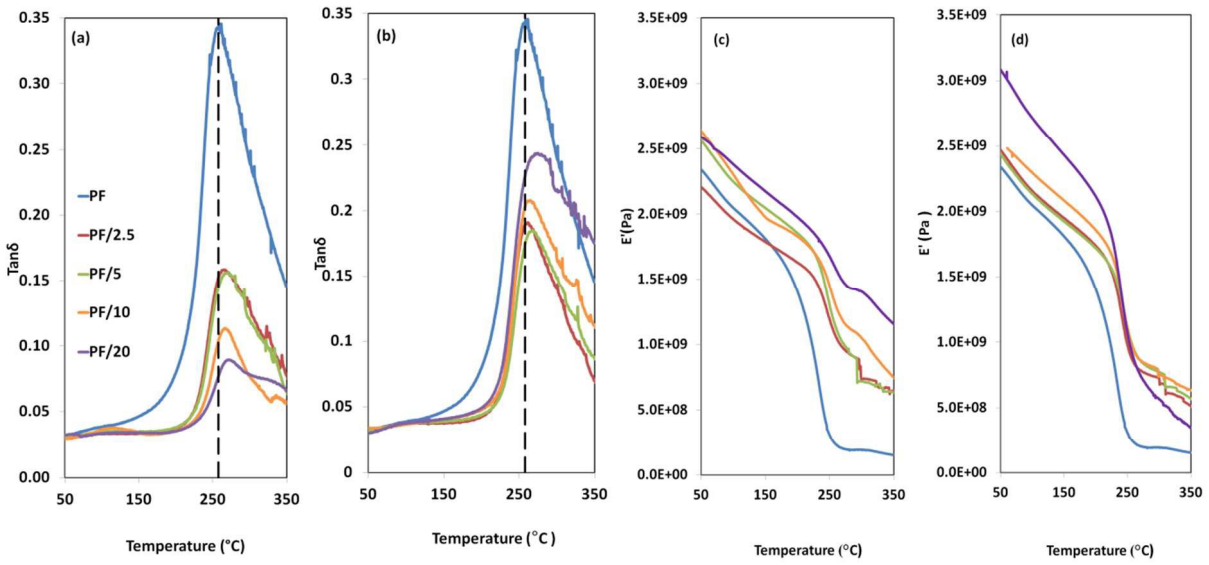

Fig. 3. DMA results obtained for fully postcured samples; (a) tanδ curve for PF/CN, (b) tanδ curve for PF/CB, (c) storage modulus curve for PF/CN and (d) storage modulus curve for PF/CB.

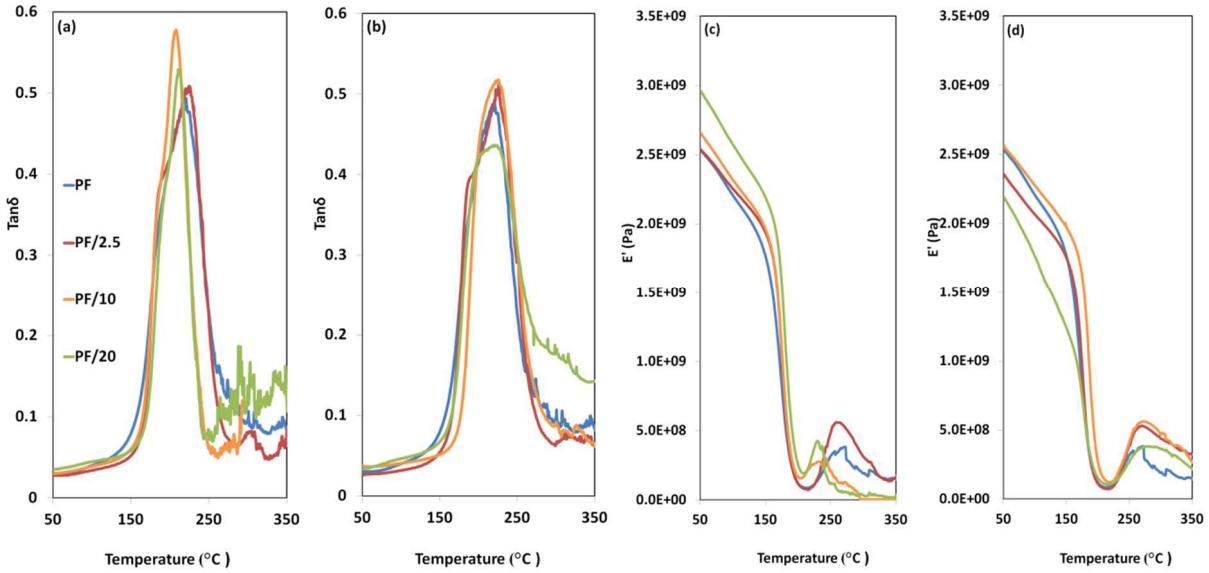

Fig. 4. DMA results obtained for fully postcured samples; (a) tanδ curve for PF/CN, (b) tanδ curve for PF/CB, (c) storage modulus curve for PF/CN and (d) storage modulus curve for PF/CB.

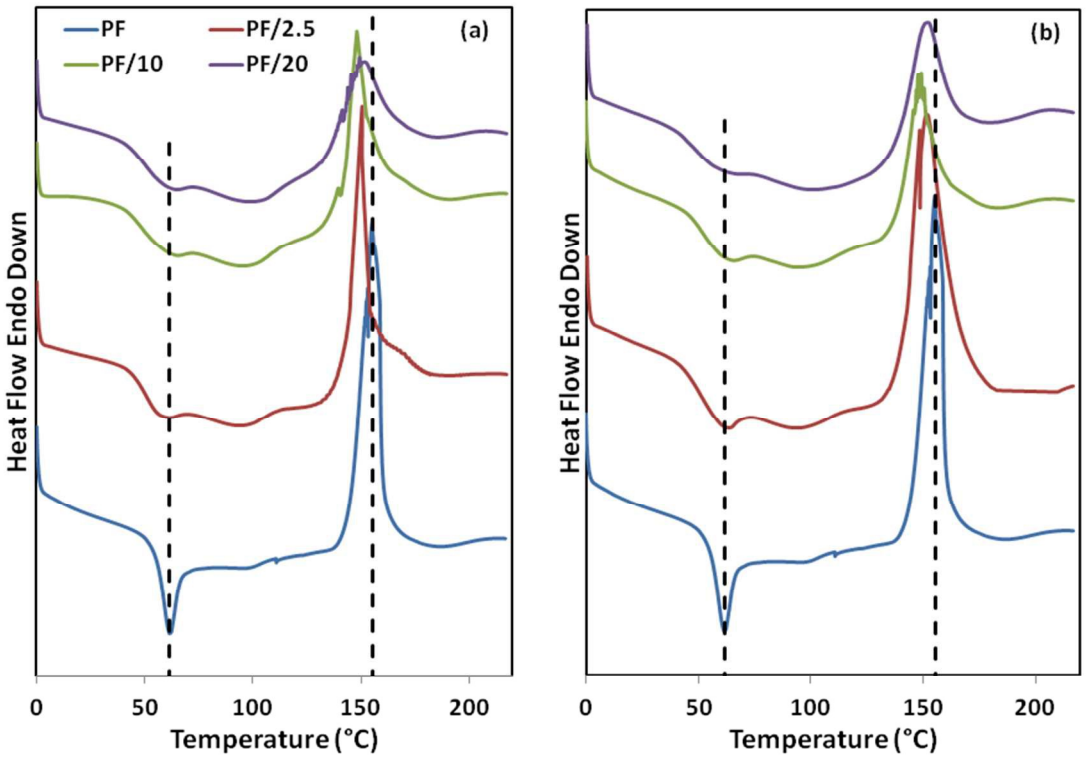

Fig. 5.DSC thermographs of uncured PF and PF/clay, (a) PF/CN and b) PF/CB.

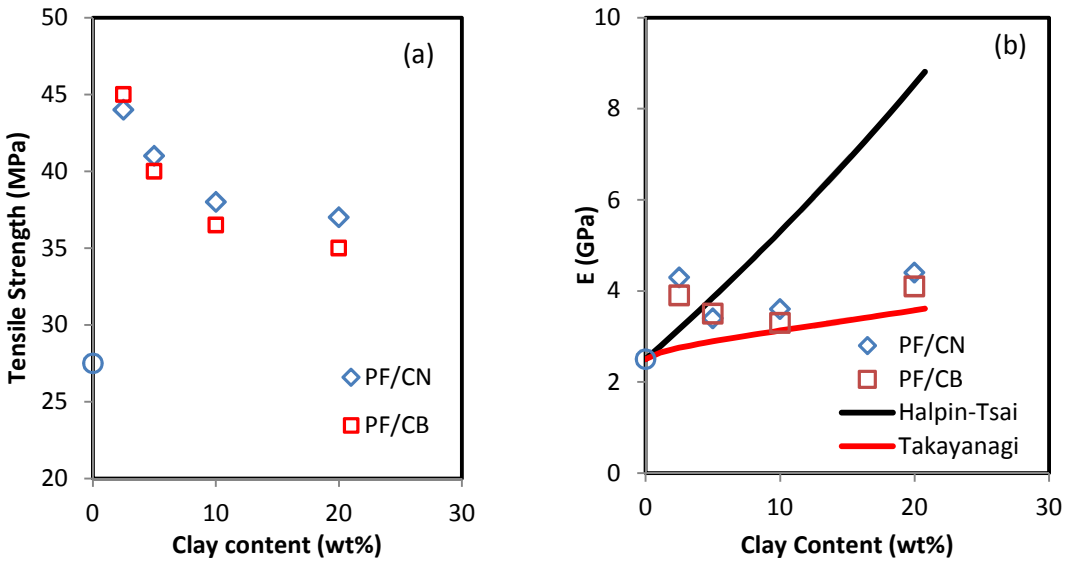

Fig. 6. Effect of clay content on the tensile properties of the fully postcured composites, (a) tensile strength and (b) tensile modulus.

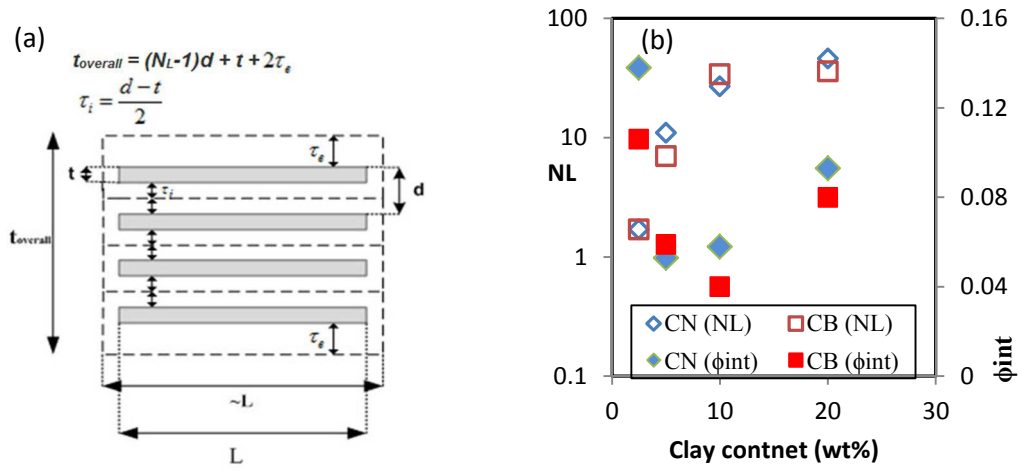

Fig. 7. (a) Schematic view of the interphase region developed around a single layer in a stack at intercalated morphology and (b) variation of N_L and interphase volume fraction (ϕ_{int}) versus clay loadings.